# Journal of Applied Meteorology and Climatology

# Teleconnections between Rainfall in Equatorial Africa and Tropical Sea-Surface Temperatures: A Focus on Western Uganda --Manuscript Draft--

Manuscript Number:	JAMC-D-21-0057
Full Title:	Teleconnections between Rainfall in Equatorial Africa and Tropical Sea-Surface Temperatures: A Focus on Western Uganda
Article Type:	Article
Corresponding Author:	Jeremy Diem Georgia State University Atlanta, Georgia UNITED STATES
Corresponding Author's Institution:	Georgia State University
First Author:	Jeremy Diem
Order of Authors:	Jeremy Diem
	Jonathan Salerno
	Michael Palace
	Karen Bailey
	Joel Hartter
Manuscript Classifications:	1.004: Africa; 4.212: ENSO; 9.020: Climate variability; 9.084: Seasonal variability; 10.052: Communications/decision making
Abstract:	Substantial research on the teleconnections between rainfall and sea-surface temperatures (SSTs) has been conducted across equatorial Africa as a whole, but currently no focused examination exists for western Uganda, a rainfall transition zone between eastern equatorial Africa (EEA) and central equatorial Africa (CEA). This study examines correlations between satellite-based rainfall totals in western Uganda and SSTs – and associated indices – across the tropics over 1983-2019. It is found that rainfall throughout western Uganda is teleconnected to SSTs in all tropical oceans, but much more strongly to SSTs in the Indian and Pacific Oceans than the Atlantic Ocean. Increased Indian Ocean SSTs during boreal winter, spring, and autumn and a pattern similar to a positive Indian Ocean Dipole during boreal summer are associated with increased rainfall in western Uganda. The most spatially complex teleconnections in western Uganda occur during September-December, with northwestern Uganda being similar to EEA during this period and southwestern Uganda being similar to CEA. During boreal autumn and winter, northwestern Uganda has increased rainfall associated with SST patterns resembling a positive Indian Ocean Dipole or El Niño. Southwestern Uganda does not have those teleconnections; in fact, increased rainfall there tends to be more associated with La Niña-like SST patterns. Tropical Atlantic Ocean SSTs also appear to influence rainfall in southwestern Uganda in boreal winter as well as in boreal summer. Overall, western Uganda is a heterogeneous region with respect to rainfall-SST teleconnections; therefore, southwestern Uganda and northwestern Uganda require separate analyses and forecasts, especially during boreal autumn and winter.

DEPARTMENT OF GEOSCIENCES

Mailing Address: P.O. Box 4105 Atlanta GA 30302-4105

In Person: 24 Peachtree Center Avenue Suite 340 Atlanta GA 30303

Phone 404/413-5750 Fax 404/413-5768



10 June 2021

Dr. Klink,

A revised version of manuscript JAMC-D-21-0057 ("Teleconnections between Western Uganda Rainfall and Tropical Sea-Surface Temperatures: A Focus on Western Uganda.") is being submitted for consideration for publication in *Journal of Applied Meteorology and Climatology*. We have made the minor changes to the manuscript as suggested by Reviewer #3. Our point-by-point response to the reviewers' comments also has been uploaded.

Sincerely

Jeremy E. Diem

Cost Estimation and Agreement Worksheet

Click here to access/download

Cost Estimation and Agreement Worksheet

Journals Estimation Worksheet.pdf

#### Reviewer #2

Comment: Original comment. L20: "- derived from satellite-based estimates-". There are a lot of usages of double hyphens in the paper. The journal could comment but I do not think this is correct. In all cases these could be replaced with parentheses, commas, restructured sentences or even just removed, without loss of meaning.

Authors' response. We prefer to follow the suggestions of the use of compound adjectives, as provided in Elements of Style.

Potential misunderstanding. In my comment I was not referring to the compound adjective (i.e. satellite-based). Instead I was referring to the enclosing hyphens (in this case appearing before "derived" and after "estimates"). Perhaps the use of these is journal-approved style; if so please discount this comment. Otherwise, alternatives are given in my original comment.

Response: Thanks for clarifying. We used em dashes in that sentence to emphasize that the rainfall data were estimated rather than measured. In the revised abstract, we use em dashes to decrease the possibility that "and associated indices" gets lost in the sentence. Em dashes were used in line 86 to place emphasis on rainfall. We used em dashes in line 279 to make certain the reader knew that the correlations were not significant. We used em dashes in line 365 to improve the readability of the sentence.

#### Reviewer #3

Comment: It would be useful to briefly comment on how different or similar CHIRPS and TAMSAT are over western Uganda as currently this isn't mentioned in this manuscript.

Response: We have modified sentences in that paragraph, and they are as follows: "For all analyses, the mean of the CHIRPS and TAMSAT values was used to decrease the impact of any errors in one of the products. CHIRPS and TAMSAT were selected because they share several important similarities: (1) have strong temporal correlations with ground-measured rainfall in western Uganda (Diem et al. 2019a); (2) extend back to at least 1983; and (3) have relatively high spatial resolutions (i.e., 0.05° for CHIRPS and 0.0375° for TAMSAT). CHIRPS was serially complete, while TAMSAT was missing 5% of daily rainfall totals."

As a result of the change described above, we have changed "The rainfall regions determined by Diem et al. (2019b) were used, and the mean of the CHIRPS and TAMSAT values was used as the rainfall total for each region" to "The rainfall regions determined by Diem et al. (2019b) were used."

Comment: Line 386: Small typo. Should be 'SST' not 'STT'.

Response: Thank you for finding that typo. It has been corrected.

Comment: Fig. 2 caption. Use of 'adjusted' still used. Needs to be removed.

Response: Thank you again. We have removed "adjusted" from the caption.

12

Teleconnections between Rainfall in Equatorial Africa and Tropical Sea-1 **Surface Temperatures: A Focus on Western Uganda** 2 3 Jeremy E. Diem, a Jonathan D. Salerno, Michael W. Palace, Karen Bailey, Joel Hartter, 4 5 <sup>a</sup> Georgia State University, Atlanta, GA 6 <sup>b</sup> Colorado State University, Fort Collins, CO <sup>c</sup> University of New Hampshire, Durham, NH 7 8 <sup>d</sup> University of Colorado, Boulder, CO 9 10 11

Corresponding author: Jeremy E. Diem, jdiem@gsu.edu

13 ABSTRACT

14

15

16

17

18

19

20

21

22

23

24

25

26

27

28

29

30

31

32

33

34

35

36

Substantial research on the teleconnections between rainfall and sea-surface temperatures (SSTs) has been conducted across equatorial Africa as a whole, but currently no focused examination exists for western Uganda, a rainfall transition zone between eastern equatorial Africa (EEA) and central equatorial Africa (CEA). This study examines correlations between satellite-based rainfall totals in western Uganda and SSTs – and associated indices – across the tropics over 1983-2019. It is found that rainfall throughout western Uganda is teleconnected to SSTs in all tropical oceans, but much more strongly to SSTs in the Indian and Pacific Oceans than the Atlantic Ocean. Increased Indian Ocean SSTs during boreal winter, spring, and autumn and a pattern similar to a positive Indian Ocean Dipole during boreal summer are associated with increased rainfall in western Uganda. The most spatially complex teleconnections in western Uganda occur during September-December, with northwestern Uganda being similar to EEA during this period and southwestern Uganda being similar to CEA. During boreal autumn and winter, northwestern Uganda has increased rainfall associated with SST patterns resembling a positive Indian Ocean Dipole or El Niño. Southwestern Uganda does not have those teleconnections; in fact, increased rainfall there tends to be more associated with La Niña-like SST patterns. Tropical Atlantic Ocean SSTs also appear to influence rainfall in southwestern Uganda in boreal winter as well as in boreal summer. Overall, western Uganda is a heterogeneous region with respect to rainfall-SST teleconnections; therefore, southwestern Uganda and northwestern Uganda require separate analyses and forecasts, especially during boreal autumn and winter.

#### SIGNIFICANCE STATEMENT

Seasonal rainfall greatly impacts the millions of rural households practicing rain-fed agriculture across equatorial Africa; therefore, understanding the relationship between rainfall

and tropical sea-surface temperatures (SSTs) can benefit smallholder farmers and other stakeholders. This study examines over the 1983-2019 period the relationships between SSTs and monthly and seasonal rainfall totals in western Uganda. During boreal spring and summer, increased SSTs in the Indian Ocean along with La Niña-like SST patterns are generally associated with increased rainfall for the entire region. Rainfall-SST relationships have substantial spatial variability during boreal autumn and winter: only northwestern Uganda has increased rainfall strongly associated with the positive Indian Ocean Dipole and El Niño-like SST patterns. These findings have implications for the region-specific forecasts provisioned to farmers.

# 1. Introduction

People throughout equatorial Africa are highly vulnerable to the impacts of rainfall variability. This region is home to millions of rural households practicing rain-fed agriculture, and their food security depends on the timing and amount of rainfall within rainy seasons (Cooper et al. 2008; Zougmoré et al. 2018). For instance, based on observation and predictions of seasonal rainfall patterns, farmers select crop types and varieties, choose where and when to plant, and apply a suite of adaptive management practices (Wilkie et al. 1999; Crane et al. 2011; Salerno et al. 2019). Drought can severely reduce food security in countries such as Kenya and Somalia (Nicholson 2014). Excessive rainfall also is detrimental to agriculture, since it increases the likelihood of crop loss due to rot and pests (Farrow et al. 2011; Okonya et al. 2013). Heavy rainfall can exacerbate soil erosion, with the 1997/1998 rainfall in Kenya associated with an El Niño event a prime example (Ngecu and Mathu 1999). Moreover, negative impacts of adverse rainfall conditions extend beyond farming; for example, excessive rainfall can exacerbate the incidence of disease such as malaria (Ssempiira et al. 2018).

Rainfall within equatorial Africa is far from uniform. Much of the western portion has the Congo rainforest with annual rainfall exceeding 1.500 mm (Todd and Washington 2004), while some places in the far eastern portion have arid climates with annual rainfall less than 600 mm (Herrmann and Mohr 2011) (Fig. 1a). Two adjacent areas for which climate has been studied at the regional scale are eastern equatorial Africa (EEA) and central equatorial Africa (CEA). These two regions differ not just in rainfall quantity but also in intra-annual characteristics of rainfall: EEA has a biannual rainfall regime (i.e., two rainy seasons), with more rainfall occurring during boreal spring (i.e., the long rains) than during boreal autumn (i.e., the short rains) (Camberlin et al. 2009; Liebmann et al. 2012), while CEA has a biannual regime but with more rainfall in boreal autumn than in boreal spring (Creese and Washington 2018). Circulation in EEA and CEA is complex, with both zonal and meridional circulations present. The Hadley circulation is comprised of meridional overturning cells and is wellstructured over the oceans, with trade winds from both hemispheres converging at the intertropical convergence zone (ITCZ), which on average is located in the Northern Hemisphere (Webster 2004; Marshall et al. 2014). Over the African continent, the ITCZ is better characterized as the tropical rain belt, since, for the most part, trade winds do not exist over Africa (Nicholson 2018). The rain belt is oriented east-to-west, migrates latitudinally, and experiences much more movement over EEA than CEA (Nicholson 2018). The Walker circulation is comprised of zonal overturning cells across the tropics, with upward motion typically present over the Congo Basin (Cook and Vizy 2016) and downward motion typically present over the western Indian Ocean and far eastern EEA (Lau and Yang 2015; King et al. 2020). Associated with the tropical rain belt is the Congo Air Boundary (CAB), which is a confluence zone oriented southwest to northeast, where westerly air from the Congo Basin meets

60

61

62

63

64

65

66

67

68

69

70

71

72

73

74

75

76

77

78

79

80

81

82

easterly air from the Indian Ocean (Nicholson 2000; Levin et al. 2009; Costa et al. 2014; Dezfuli 2017).

El Niño Southern Oscillation (ENSO) and the Indian Ocean Dipole (IOD) are oscillations of tropical sea-surface temperatures (SSTs) that impact the Walker circulation – and ultimately rainfall – over EEA and CEA. Surface westerlies are typical across the Indian Ocean (Hastenrath and Polzin 2004), and those westerlies prevail across the Indian Ocean during a La Niña event (Lau and Yang 2015). During an El Niño event, there is a weakening of the Indian Ocean Walker cell and thus a shift to easterly winds across the Indian Ocean (Camberlin et al. 2001; Lau and Yang 2015). High (low) SSTs in the western Indian Ocean and low (high) SSTs in the southeastern Indian Ocean represent positive (negative) IOD events (Saji et al. 1999). Hereafter, positive IOD and negative IOD will be referred to as pIOD and nIOD, respectively. A pIOD event forces anomalous southeasterly trade winds that increase moisture supply into EEA from the Indian Ocean (Black et al. 2003; Liebmann et al. 2014). pIOD events often co-occur with El Niño events (Schott et al. 2007), with El Niño possibly predisposing the Indian Ocean coupled system to a pIOD event (Black et al. 2003).

#### a. Rainfall teleconnections with SSTs

#### 1) INDIAN OCEAN

Increased SSTs in the Indian Ocean, particularly in the western portion, tend to be teleconnected (i.e., connected across a large geographical scale) to increased rainfall in both EEA and CEA. There are nonexistent to weakly positive correlations between boreal-spring rainfall in both EEA and CEA and Indian Ocean SSTs (Nicholson and Dezfuli 2013; Omondi et al. 2013; Lyon 2014; Vellinga and Milton 2017). The IOD becomes a factor in boreal summer and autumn in EEA: pIOD-like patterns are positively correlated with rainfall in southeastern Ethiopia during

boreal summer (Dubache et al. 2019) and with rainfall throughout EEA during boreal autumn (Black et al. 2003; Lyon 2014; Bahaga et al. 2015; Nicholson 2015; Wenhaji Ndomeni et al. 2017; Endris et al. 2019). While rainfall in CEA is not strongly correlated with Indian Ocean SSTs in boreal summer (Creese and Washington 2016), there is increased rainfall in boreal autumn in far eastern CEA when the western Indian Ocean is warmer (Dezfuli and Nicholson 2013).

#### 2) PACIFIC OCEAN

106

107

108

109

110

111

112

113

114

115

116

117

118

119

120

121

122

123

124

125

126

127

128

129

Wet boreal winters and autumns in EEA are teleconnected to El Niño-like SST patterns, wet boreal springs have relatively weak teleconnections to tropical Pacific Ocean SSTs, and wet boreal summers are teleconnected to La Niña-like SST patterns. While few studies focus on boreal winter, the season is likely wetter (drier) over the region during El Niño (La Niña) years (de Oliveira et al. 2018). There has been much more research on the teleconnections between ENSO and the "short rains" of boreal autumn, with the major findings that El Niño (La Niña) leads to increased (decreased) rainfall (Mutai and Ward 2000; Camberlin et al. 2001; Black et al. 2003; Schreck and Semazzi 2004; Lyon 2014; Wenhaji Ndomeni et al. 2017; Endris et al. 2019). In addition, EEA may receive increased rainfall only when El Niño occurs synchronously with a pIOD event (Black 2003; Behera et al. 2005; Bahaga et al. 2015; MacLeod et al 2020). During boreal spring, there are weak negative correlations between rainfall and SSTs in the central and eastern equatorial Pacific Ocean (Camberlin et al. 2001; Camberlin and Phillipon 2002; Endris et al. 2019). Weak positive correlations between rainfall and central equatorial Pacific Ocean SSTs also have been found for boreal spring (Lyon 2014). Strong negative correlations between rainfall and central and eastern equatorial Pacific Ocean SSTs exist during boreal summer (Camberlin et al. 2001; Segele et al. 2009; Berhane et al. 2014; Lyon 2014; Degefu et al. 2017; Gleixner et al. 2017; de Oliveira et al. 2018; Endris et al. 2019).

CEA generally has increased rainfall teleconnected to La Niña-like SST patterns (i.e., decreased rainfall and El Niño-like SST patterns). Rainfall is positively correlated with La Niña-like patterns during boreal winter (Balas et al. 2007), boreal spring (Camberlin et al. 2001; Nicholson and Dezfuli 2013), and boreal summer (Balas et al. 2007; Endris et al. 2019). Rainfall in the far eastern portion during boreal autumn, specifically October-December, appears to be positively correlated with El Niño-like SST patterns (Dezfuli and Nicholson 2013). However, pure El Niño events (i.e., no connection to an IOD phase) are associated with decreased rainfall during September-November (Bahaga et al. 2015).

# 3) ATLANTIC OCEAN

Teleconnections between Atlantic Ocean SSTs and seasonal rainfall in EEA and CEA are not especially strong. Throughout most of EEA there are no significant correlations between rainfall and tropical Atlantic Ocean SSTs (Camberlin et al. 2001; Degefu et al. 2017). Boreal-spring rainfall in CEA is positively (negatively) correlated with tropical south (north) Atlantic SSTs; the positive correlation also includes Gulf of Guinea SSTs (Nicholson and Dezfuli 2013). Warm SST anomalies in the southern tropical Atlantic Ocean are associated with wet (dry) boreal summers (winters) in CEA (Balas et al. 2007). There is likely no connection between Atlantic Ocean SSTs and CEA rainfall during boreal autumn (Creese and Washington 2018).

#### b. Purpose and objectives of study

Western Uganda is an important area to focus on for several reasons. First, since western Uganda is transitional between EEA and CEA with respect to rainfall (Monaghan et al. 2012; Diem et al. 2019a), detailed analyses of tropical SST teleconnections with rainfall in the region fills a critical gap in our understanding of the climate of equatorial Africa. Currently, only rough estimates of teleconnections have been deduced based on results from EEA and CEA studies.

Second, millions of people (with some of the most concentrated and fastest growing human populations on the planet) depend on rainfed agriculture for livelihoods in western Uganda (Diem et al. 2017), and those smallholder farmers currently desire more accurate seasonal rainfall forecasts from the government (Osbahr et al. 2011; Roncoli et al 2011) and might be becoming increasingly reliant on seasonal forecasts in the future (Roncoli et al. 2002). Rainfall-SST teleconnections play an important role in the forecasts the Uganda National Meteorological Authority (UNMA) produces for regions within Uganda: those forecasts are based largely on IOD and ENSO conditions (UNMA 2021). Third, western Uganda has likely had increasing rainfall trends in all seasons except for boreal winter (Diem et al. 2019a,b) – which makes it unique within equatorial Africa – and understanding rainfall-SST teleconnections will provide a foundation for future research that attempts to understand the wetting trend in the region.

The purpose of this research is to better understand how rainfall in western Uganda is

teleconnected to tropical SSTs of the Indian, Pacific, and Atlantic Oceans. The study involves months in addition to seasons, because existing studies have used a variety of season definitions (e.g., September-November and October-November for boreal autumn) and – as Nicholson (2016) notes – there can be markedly different teleconnections among the months within a season. The objectives for this study are as follows: (1) identify statistically significant teleconnections between seasonal and monthly rainfall and concurrent tropical SSTs and associated indices; and (2) examine the spatial complexity of the intra-annual variability in teleconnections.

# 2. Study Area

Western Uganda has rainfall totals and seasonal rainfall variability that are transitional between EEA and CEA (Figs. 1 and 2). Diem et al. (2019b) divided western Uganda into five

homogeneous rainfall regions that represented latitudinal zones as well as a western region, Region 3, that is a small portion of lowland rainforest extending into the Congo Basin. Annual rainfall totals for the five regions ranges from ~1,100 to ~1,400 mm (Fig. 2). These rainfall totals are higher than the mean for EEA (Nicholson 2017), but lower than the mean for CEA (Todd and Washington 2004). Region 1, the northernmost region, exists between 2 °N and 4 °N latitude and has an annual rainfall regime, with the one long rainy season occurring from late March to mid-November. The rest of the regions are much closer to the equator and have biannual rainfall regimes, with the first rainy season typically occurring from mid-March to mid-May and the second rainy season occurring from August through November. Region 5, the southernmost region, has slightly different rainy seasons than the other regions with a biannual regime: the first rains begin earlier (i.e., March 1) and the second rains start later (i.e., late August) and end later (i.e., early December). For the four regions with a biannual rainfall regime, the second rains are approximately 50 days longer (i.e., 116 days vs. 66 days) than the first rains. Consequently, in contrast to most parts of EEA, the first rains in western Uganda are called the "short rains" and second rains are called the "long rains" (Hartter et al. 2012; Diem et al. 2017).

#### 3. Data and Methods

176

177

178

179

180

181

182

183

184

185

186

187

188

189

190

191

192

193

194

195

196

197

198

Rainfall data consisted of satellite-based rainfall estimates from two rainfall products. Daily estimates for 1983-2019 from version 2 of CHIRPS (Climate Hazards Group InfraRed Precipitation with Stations) (Funk et al. 2015) and version 3 of TAMSAT (Tropical Applications of Meteorology using SATellite and ground based observations) (Maidment et al. 2017) were obtained from the International Research Institute for Climate and Society at Columbia University. For all analyses, the mean of the CHIRPS and TAMSAT values was used to decrease the impact of any errors in one of the products. CHIRPS and TAMSAT were selected because

they share several important similarities: (1) have strong temporal correlations with groundmeasured rainfall in western Uganda (Diem et al. 2019a); (2) extend back to at least 1983; and (3) have relatively high spatial resolutions (i.e., 0.05° for CHIRPS and 0.0375° for TAMSAT). CHIRPS was serially complete, while TAMSAT was missing 5% of daily rainfall totals. For each of those 678 days with missing data, the mean value for the day of year was used as the predicted rainfall total. Tropical-SST data included gridded SSTs and associated indices. Gridded SST data were extracted from the Optimal Interpolation SST Analysis, Version 2 (OISSTV2) (Reynolds et al. 2002): the data were acquired from the National Oceanic and Atmospheric Administration (NOAA). The data have 1° spatial resolution. The Indian Ocean SST indices consisted of the WTIO (Western Tropical Indian Ocean) index, the SETIO (Southeastern Tropical Indian Ocean) index, and the DMI (Dipole Mode Index). The DMI, the difference between the WTIO and SETIO indices, is an indicator of the Indian Ocean Dipole (Saji et al. 1999). The Pacific Ocean indices consisted of the Western Pacific (WP) index, the Niño4 index, the Niño 3.4 index, the Niño 3 index, the Niño 1+2 index, and the Southern Oscillation Index (SOI). The OISSTV2 data was used to calculate the WP index, which is the mean SST within 0° to 10° N and 130° to 150° W (Hoell and Funk 2013). The Atlantic Ocean SST indices consisted of the North Atlantic Tropical (NAT) index, the South Atlantic Tropical (SAT) index, and the Tropical Atlantic Meridional Gradient (TAMG) index. The TAMG, the difference between the NAT and SAT indices, is an indicator of the meridional SST gradient in the tropical Atlantic Ocean and thus the north-south displacement of the Atlantic ITCZ (Chang et al. 1997; Mélice and Servain 2003). The spatial domains of the SST indices described above are shown on Fig. 3. All indices except

199

200

201

202

203

204

205

206

207

208

209

210

211

212

213

214

215

216

217

218

219

220

221

for WP were acquired from NOAA.

Temporal correlations between rainfall and SSTs and associated indices were calculated from 1983-2019. The rainfall regions determined by Diem et al. (2019b) were used, and the mean of the CHIRPS and TAMSAT values was used as the rainfall total for each region. Correlations were calculated for each region-month combination and each region-season combination. The selected months corresponding to boreal winter, spring, summer, and autumn were December-February (DJF), March-May (MAM), June-August (JJA), and September-November (SON), respectively. These seasons generally match the seasons used in other rainfall-SST studies across equatorial Africa, thereby enabling a comparison of findings. In addition, DJF and JJA encapsulate dry seasons for much of the region and MAM and SON encapsulate rainy seasons (Fig. 2). All time series (i.e., rainfall, SSTs, and indices) were detrended using the trend line from linear regression (e.g., Lyon 2014), and all subsequent analyses were performed using residuals. The detrending removes spurious correlations created by trends (e.g., Bahaga et al. 2015). Correlations were assessed using Pearson product- moment correlation tests ( $\alpha = 0.05$ ; two tailed). The temporal correlations were used to assess the intra-annual variability in inter-regional differences in rainfall-SST teleconnections. Absolute differences in correlations were calculated for each month-index combination for ten pairs of regions. The mean absolute difference was then calculated from the ten values. The mean absolute differences were then found for the Indian Ocean (WTIO, SETIO, and DMI), Pacific Ocean (WP, Niño4, Niño3.4, Niño3, Niño1+2, and SOI), and Atlantic Ocean (NAT, SAT, and TAMG).

222

223

224

225

226

227

228

229

230

231

232

233

234

235

236

237

238

239

240

241

# 4. Results

242

243

244

245

246

247

248

249

250

251

252

253

254

255

256

257

258

259

260

261

262

263

a. Seasonal teleconnections with Indian Ocean SSTs

Increased DJF rainfall in all regions was associated with high SSTs across the Indian Ocean, especially the western portion (Figs. 4a-e and 5). All regions had significant positive correlations with SSTs in the western Indian Ocean, and all but Regions 3 and 4 had significant correlations with the WTIO index. Regions 1 and 2 also had significant positive correlations with the SETIO index. Regions 1 and 5 had significant positive correlations with the DMI. Increased MAM rainfall in all regions was associated with high SSTs across the Indian Ocean, but the correlations were much weaker compared to those during DJF (Figs. 4f-j and 5b). None of the regions had rainfall significantly correlated with the WTIO and SETIO indices; however, Regions 3 and 5 did have significant negative correlations with the DMI. pIOD-like patterns were associated with increased rainfall in western Uganda during boreal summer (Figs. 4k-o and 5d). All regions had significant positive correlations in parts of the western tropical Indian Ocean and all regions but Region 1 had significant negative correlations in parts of the southeastern tropical Indian Ocean. However, only Region 4 had a significant positive correlation with the DMI. Increased SON rainfall in all regions was strongly associated with SSTs across the Indian Ocean, with a pIOD-like pattern linked to Region 1 (Figs. 4p-t and 5d). Apart from Region 1, none of the regions had strong correlations with the Indian Ocean indices. While Region 1 did have strong positive correlations with the WTIO index and the DMI and a strong negative correlation with the SETIO index, none of the correlations were significant. All regions had

significant positive correlations with SSTs in the far southeastern Indian Ocean (i.e., south of the

SETIO index region). And Region 3 had significant negative correlations with SSTs in the southwestern tropical Indian Ocean.

b. Seasonal teleconnections with Pacific Ocean SSTs

Increased DJF rainfall for all regions except Region 3, the westernmost region, was associated with El Niño-like SST patterns, but Region 1 was the only region with significant correlations (Figs. 4a-e and 5a). While all regions had negative correlations with SSTs in the western tropical Pacific Ocean, only Regions 1 and 2 had significant correlations with the WP index. Region 1 also was the only region with significant positive correlations with any of the Niño indices and an associated significant negative correlation with the SOI.

MAM rainfall was generally weakly correlated with western Pacific Ocean SSTs, with most regions having increased rainfall associated with weak La Niña-like SST patterns (Figs. 4f-j and 5b). Region 1 had significant positive correlations with SSTs in the Niño4 region, but the correlation with the Niño4 index was not significant. While most of the regions had strong negative correlative correlations with SSTs in the eastern tropical Pacific Ocean, only Region 2 had a significant negative correlation with an associated Niño index.

JJA rainfall for all regions was negatively correlated with central Pacific Ocean SSTs for all regions (Figs. 4k-o and 5d). Only Regions 1, 2, and 3 had significant correlations with at least one Niño index. Regions 1 and 2 also had strong – but not significant – positive correlations with the SOI.

Only the two southernmost regions had strong correlations between SON rainfall and Pacific Ocean SSTs, and increased rainfall in those two regions was associated with La Niña-like SST patterns (Figs. 4p-t and 5d). Regions 4 and 5 had significant negative correlations with central Pacific Ocean SSTs, and thus the Niño4, Niño3.4, Niño3 indices along with the SOI, and

significant positive correlations with the western Pacific Ocean SSTs and the associated WP index. Regions 1, 2, and 3 had weak correlations with SSTs and the indices.

#### c. Teleconnections with Atlantic Ocean SSTs

DJF rainfall in all regions was positively associated with SSTs in the north Atlantic Ocean and the Gulf of Guinea (Figs. 4a-e and 5a). All regions had strong correlations with the NAT index, but only Regions 3, 4, and 5 had significant positive correlations. These three regions also had significant positive correlations with the TAMG index.

In contrast to the situation for DJF, there were mostly weak teleconnections between regional rainfall and Atlantic Ocean SSTs for the other seasons (Figs. 4k-t and 5b-d). During MAM, significant negative correlations existed across the ocean, particularly in the southern portion (Fig. 4k-o and 5b). However, none of the correlations with the indices were significant (Fig. 5b). There were mostly positive correlations between rainfall and SSTs during JJA, but none of the SST or index correlations were significant. Except for Region 3 during SON, there were no significant correlations between rainfall and indices (Fig. 5d). Region 3 had a significant negative correlation with SSTs in the south Atlantic Ocean and significant positive correlations with SSTs in the north Atlantic Ocean, and by extension there were significant negative and positive correlations with the SAT and TAMG indices, respectively (Fig. 4p-t and 5d).

# d. Intra-annual variability in spatial complexity of teleconnections

Differences among the regions in teleconnections were maximized in October and in general largest during September-December (Figs. 6 and 7). The October peak in differences for the Indian Ocean was the largest of all the differences: the October mean absolute difference in correlations was twice as large as that for the month with second-largest difference. The differences for the Pacific Ocean generally increased from January to October.

There were substantial shifts in teleconnections during September-December (i.e., the period with the largest differences in teleconnections among the regions) (Figs. 7 and 8). September rainfall, especially for Regions 1 and 2, was positively correlated with La Niña-like SST patterns (Fig. 8a,b). These patterns also prevailed in July and August, especially for the northern regions (Fig. 7). The teleconnections in Regions 1 and 2 were transitioning in October: those regions had rainfall positively correlated with pIOD-like patterns and weak El Niño-like patterns (Fig. 8 f,g). The southern regions had nearly the opposite teleconnections (Fig. 8 h-j). In November and December, rainfall in Regions 1 and 2 was positively correlated with both an El Niño-like SST pattern and a pIOD-like SST pattern (Fig. 8 k,l,p,q). The southern regions had much weaker versions of those teleconnections.

# 5. Discussion

#### a. Boreal-winter teleconnections

Uganda. A warm western Indian Ocean, and to a lesser degree a pIOD-like pattern, are associated with increased rainfall in all regions, and this also has been found for rainfall over all of CEA (Creese and Washington 2016). El Niño-like patterns were positively correlated with rainfall in the northern regions of western Uganda, but these patterns are limited to December and are thus not representative of the entire season. Nevertheless, it is wetter over EEA during El Niño years (de Oliveira et al. 2018); therefore, Region 1 during DJF appears to be an extension of EEA. Rainfall in Region 3, which is 175 km to the west of Region 1 and is essentially in the eastern Congo Basin, does not have any connection with El Niño-like patterns. The lack of a teleconnection with ENSO in the eastern Congo Basin is expected, since decreased rainfall on the western side of the basin is associated with El Niño-like patterns (Nicholson and Kim 1997;

Camberlin et al. 2001). The southern regions (e.g., Regions 4 and 5) also have increased rainfall associated with a warm (cool) northern (southern) tropical Atlantic Ocean. The tropical Atlantic Ocean also is a control of CEA rainfall, with the negative SST anomalies in the southern tropical Atlantic Ocean presumed to keep the rain belt near the equator (Balas et al. 2007).

# b. Boreal-spring teleconnections

Among the seasons, boreal spring has the weakest teleconnections between rainfall in western Uganda and tropical SSTs. Western Uganda seems to be more similar to the eastern Congo than EEA during boreal spring: the eastern Congo Basin also has rainfall positively correlated with SSTs in the western Indian Ocean or a pIOD-like SST pattern (Nicholson and Dezfuli 2013), while for EEA there are weak correlations and mixed results (Omondi et al. 2013; Lyon 2014; Vellinga and Milton 2017). There does not appear to be a clear La Niña-like or El Niño-like pattern associated with increased rainfall in EEA (Camberlin et al. 2001; Camberlin and Phillipon 2002; Endris et al. 2019; Lyon 2014), but CEA is similar to western Uganda in that La Niña-like patterns are positively correlated with rainfall (Camberlin et al. 2001; Nicholson and Dezfuli 2013). Finally, western Uganda is like EEA in that it has weak correlations with tropical Atlantic Ocean SSTs, while there are stronger correlations in CEA (Nicholson and Dezfuli 2013).

#### c. Boreal-summer teleconnections

pIOD-like SST patterns, La Niña-like SST patterns, and an anomalously warm southern

Atlantic Ocean are teleconnected to increased rainfall in western Uganda during boreal summer.

If the months constituting this season are July-September rather than June-August, then the La

Niña teleconnection becomes much stronger. The pIOD-like pattern is important for all regions,

while the La Niña pattern is more important for the northern regions. EEA generally also has the

pIOD-like pattern (Dubache et al. 2019) and a La Niña-like pattern (Camberlin et al. 2001; Segele et al. 2009; Lyon 2014; Gleixner et al. 2017; de Oliveira et al. 2018; Endris et al. 2019) associated with more rainfall. CEA rainfall as a whole is not associated with IOD-like patterns, but – similar to western Uganda and EEA – rainfall in CEA is positively correlated with La Niña-like patterns (Creese and Washington 2016). Rainfall in August and September is correlated with southern Atlantic Ocean SSTs, and a warmer southern Atlantic Ocean should keep the rain belt closer to the equator during boreal summer (Balas et al. 2007).

#### d. Boreal-autumn teleconnections

356

357

358

359

360

361

362

363

364

365

366

367

368

369

370

371

372

373

374

375

376

377

378

379

Boreal autumn has the most spatially complex teleconnections across western Uganda, with the northern regions similar to EEA and the southern regions similar to CEA. While for Region 1 – and to a lesser degree Region 2 – rainfall is positively correlated with both pIOD-like and El Niño-like SST patterns for September-November and October-December, the teleconnections are stronger for the latter group of months. The strongest teleconnections are in November and December. El Niño-like or pIOD-like patterns or both also lead to increased rainfall in EEA (Mutai and Ward 2000; Camberlin et al. 2001; Black et al. 2003; Schreck and Semazzi 2004; Behera et al. 2005; Lyon 2014; Bahaga et al. 2015; Wenhaji Ndomeni et al. 2017; Endris et al. 2019). The southern regions do have rainfall positively correlated with Indian Ocean SSTs (but not a pIOD-like pattern). The same relationship with Indian Ocean SSTs has been found for CEA (Dezfuli and Nicholson 2013). Only when September is included as part of boreal autumn does the rest of western Uganda have strong correlations between rainfall and Pacific Ocean SSTs. Rainfall is teleconnected to a La Niña-SST pattern. Neither during September-November, October-December, nor any of the months individually do the southern regions have significant correlations between rainfall and El Niño-like SST patterns. This finding is similar to what was found for CEA in Endris et al. (2019), but it contrasts with results in Dezfuli and Nicholson

(2013) showing a strong positive correlation between rainfall in far eastern CEA and El Niño-like SST patterns. The contrast may be due to the much larger latitudinal extent (i.e., 15 degrees) of the region in Dezfuli and Nicholson (2013). Finally, while rainfall in western Uganda is positively correlated with northern tropical Atlantic Ocean SSTs and negatively correlated with southern Atlantic Ocean SSTs, the lack of research on Atlantic Ocean teleconnections and rainfall in EEA and CEA makes it difficult to contextualize these findings.

# 6. Conclusions

380

381

382

383

384

385

386

387

388

389

390

391

392

393

394

395

396

397

398

399

400

401

402

There is considerable intra-annual and inter-regional variability in rainfall-SST teleconnections for western Uganda, which has traditionally been considered to have rainfall totals and seasonal rainfall variability that are transitional between EEA and CEA. Based on teleconnections, northwestern Uganda and southwestern Uganda are more similar to EEA and CEA, respectively. Rainfall throughout western Uganda is teleconnected to SSTs in all tropical oceans, but much more so to SSTs in the Indian and Pacific Oceans than the Atlantic Ocean. Increased Indian Ocean SSTs during boreal winter, spring, and autumn and a pIOD-like pattern during boreal summer are associated with increased rainfall throughout western Uganda, and this is generally true for both EEA and CEA. During boreal autumn and winter, only northwestern Uganda has increased rainfall associated with a pIOD-like pattern or an El Niño-like SST pattern. Southwestern Uganda does not have these teleconnections, therefore, it would be a mistake assuming that either the IOD or ENSO or both have a significant impact on rainfall there during September-December. In fact, Atlantic Ocean SSTs, which might be overlooked by seasonal forecasters in the region, appear to impact rainfall in southwestern Uganda in boreal winter and summer, which aligns with what has been found for CEA. Future studies should extend this work over a much larger geographic scale (e.g., all of equatorial Africa) to determine

403 the extent of the rainfall-SST teleconnection zone that includes southwestern Uganda and the 404 spatial gradient in teleconnections that exist across the Congo Basin, which has been much less 405 studied compared to East Africa. 406 Acknowledgments. 407 This research was supported by the National Science Foundation (award number 1740201) 408 and approved by the Uganda National Council for Science and Technology. 409 Data Availability Statement. 410 All gridded rainfall data, SST data, and indices data used in this study are publicly available. 411 CHIRPS and TAMSAT, the gridded rainfall products, were obtained from the International 412 Research Institute for Climate and Society and are available at https://iridl.ldeo.columbia.edu/. 413 OISSTV2 data (i.e., gridded SST data) were obtained from the National Oceanic and 414 Atmospheric Administration and are available at 415 https://psl.noaa.gov/data/gridded/data.noaa.oisst.v2.highres.html. All SST indices and the SOI 416 were obtained from NOAA and are available at https://stateoftheocean.osmc.noaa.gov. Daily 417 rainfall data for the rainfall regions in this manuscript—as well as geo-spatial data for the 418 regions—can be accessed at https://data.mendeley.com/datasets/ppxktx233y/2. 419 REFERENCES 420

Bahaga, T. K., G. Mengistu Tsidu, F. Kucharski, and G. T. Diro, 2015: Potential predictability of the sea-surface temperature forced equatorial East African short rains interannual variability in the 20th century. *Quarterly Journal of the Royal Meteorological Society*, **141**, 16–26, https://doi.org/10.1002/qj.2338.

421

422

423

- Balas, N., S. E. Nicholson, and D. Klotter, 2007: The relationship of rainfall variability in West
- 425 Central Africa to sea-surface temperature fluctuations. *International Journal of Climatology*,
- 426 **27**, 1335–1349, <a href="https://doi.org/10.1002/joc.1456">https://doi.org/10.1002/joc.1456</a>.
- 427 Behera, S. K., J.-J. Luo, S. Masson, P. Delecluse, S. Gualdi, A. Navarra, and T. Yamagata, 2005:
- Paramount impact of the Indian Ocean Dipole on the East African short rains: A CGCM
- 429 Study. *Journal of Climate*, **18**, 4514–4530, https://doi.org/10.1175/JCLI3541.1.
- Berhane, F., B. Zaitchik, and A. Dezfuli, 2014: Subseasonal analysis of precipitation variability
- in the Blue Nile River Basin. Journal of Climate, 27, 325–344, https://doi.org/10.1175/JCLI-
- 432 D-13-00094.1.
- Black, E., 2005: The relationship between Indian Ocean sea–surface temperature and East
- 434 African rainfall. Philosophical Transactions of the Royal Society A: Mathematical, Physical
- 435 and Engineering Sciences, 363, 43–47, https://doi.org/10.1098/rsta.2004.1474.
- 436 —, J. Slingo, and K. R. Sperber, 2003: An observational study of the relationship between
- excessively strong short rains in coastal East Africa and Indian Ocean SST. *Monthly Weather*
- 438 Review, **131**, 74–94, https://doi.org/10.1175/1520-
- 439 0493(2003)131<0074:AOSOTR>2.0.CO;2.
- Cai, W., A. Santoso, G. Wang, E. Weller, L. Wu, K. Ashok, Y. Masumoto, and T. Yamagata,
- 2014: Increased frequency of extreme Indian Ocean Dipole events due to greenhouse
- warming. *Nature*, **510**, 254–258, <a href="https://doi.org/10.1038/nature13327">https://doi.org/10.1038/nature13327</a>.
- 443 Camberlin, P., and N. Philippon, 2002: The East African March–May rainy season: Associated
- atmospheric dynamics and predictability over the 1968–97 period. *Journal of Climate*, **15**,
- 445 1002–1019, https://doi.org/10.1175/1520-0442(2002)015<1002:TEAMMR>2.0.CO;2.

- 446 —, S. Janicot, and I. Poccard, 2001: Seasonality and atmospheric dynamics of the
- teleconnection between African rainfall and tropical sea-surface temperature: Atlantic vs.
- ENSO. International Journal of Climatology, 21, 973–1005, https://doi.org/10.1002/joc.673.
- 449 —, V. Moron, R. Okoola, N. Philippon, and W. Gitau, 2009: Components of rainy seasons'
- variability in Equatorial East Africa: Onset, cessation, rainfall frequency and intensity.
- 451 Theoretical and Applied Climatology, **98**, 237–249, https://doi.org/10.1007/s00704-009-
- 452 0113-1.
- Chang, P., L. Ji, and H. Li, 1997: A decadal climate variation in the tropical Atlantic Ocean from
- 454 thermodynamic air-sea interactions. *Nature*, 385, 516–518,
- 455 <u>https://doi.org/10.1038/385516a0</u>.
- 456 Cook, K. H., and E. K. Vizy, 2016: The Congo Basin Walker circulation: Dynamics and
- 457 connections to precipitation. *Climate Dynamics*, **47**, 697–717,
- 458 https://doi.org/10.1007/s00382-015-2864-y.
- Cooper, P. J. M., J. Dimes, K. P. C. Rao, B. Shapiro, B. Shiferaw, and S. Twomlow, 2008:
- 460 Coping better with current climatic variability in the rain-fed farming systems of sub-Saharan
- Africa: An essential first step in adapting to future climate change? *Agriculture, Ecosystems*
- 462 & Environment, 126, 24–35, https://doi.org/10.1016/j.agee.2008.01.007.
- 463 Costa, K., J. Russell, B. Konecky, and H. Lamb, 2014: Isotopic reconstruction of the African
- Humid Period and Congo Air Boundary migration at Lake Tana, Ethiopia. *Quaternary*
- 465 *Science Reviews*, **83**, 58–67, <a href="https://doi.org/10.1016/j.quascirev.2013.10.031">https://doi.org/10.1016/j.quascirev.2013.10.031</a>.
- 466 Crane, T. A., C. Roncoli, and G. Hoogenboom, 2011: Adaptation to climate change and climate
- variability: The importance of understanding agriculture as performance. NJAS Wageningen
- Journal of Life Sciences, **57**, 179–185, https://doi.org/10.1016/j.njas.2010.11.002.

469 Creese, A., and R. Washington, 2016: Using afflux to constrain modeled Congo Basin rainfall in 470 the CMIP5 ensemble. Journal of Geophysical Research: Atmospheres, 121, 13,415-13,442, 471 https://doi.org/10.1002/2016JD025596. 472 —, and ——, 2018: A process-based assessment of CMIP5 rainfall in the Congo Basin: The 473 September–November rainy season. *Journal of Climate*, **31**, 7417–7439, 474 https://doi.org/10.1175/JCLI-D-17-0818.1. 475 de Oliveira, C. P., L. Aímola, T. Ambrizzi, and A. C. V. Freitas, 2018: The Influence of the 476 regional Hadley and Walker circulations on precipitation patterns over Africa in El Niño, La 477 Niña, and neutral years. Pure and Applied Geophysics, 175, 2293–2306, 478 https://doi.org/10.1007/s00024-018-1782-4. 479 Degefu, M. A., D. P. Rowell, and W. Bewket, 2017: Teleconnections between Ethiopian rainfall 480 variability and global SSTs: observations and methods for model evaluation. *Meteorology* 481 and Atmospheric Physics, 129, 173–186, https://doi.org/10.1007/s00703-016-0466-9. 482 Dezfuli, A. K., and S. E. Nicholson, 2013: The relationship of rainfall variability in western 483 equatorial Africa to the tropical oceans and atmospheric circulation. Part II: The boreal 484 autumn. Journal of Climate, 26, 66–84, https://doi.org/10.1175/JCLI-D-11-00686.1. 485 Dezfuli, A., 2017: Climate of western and central equatorial Africa. Oxford Research 486 Encyclopedia of Climate Science, Oxford University Press. 487 Diem, J. E., J. Hartter, J. Salerno, E. McIntyre, and A. Stuart Grandy, 2017: Comparison of 488 measured multi-decadal rainfall variability with farmers' perceptions of and responses to 489 seasonal changes in western Uganda. Regional Environmental Change, 17, 1127–1140, 490 https://doi.org/10.1007/s10113-016-0943-1.

-, B. L. Konecky, J. Salerno, and J. Hartter, 2019a: Is equatorial Africa getting wetter or 491 492 drier? Insights from an evaluation of long- term, satellite- based rainfall estimates for 493 western Uganda. International Journal of Climatology, 39, 3334–3347, 494 https://doi.org/10.1002/joc.6023. -, H. S. Sung, B. L. Konecky, M. W. Palace, J. Salerno, and J. Hartter, 2019b: Rainfall 495 496 characteristics and trends—and the role of Congo westerlies—in the western Uganda 497 transition zone of equatorial Africa from 1983 to 2017. Journal of Geophysical Research: 498 Atmospheres, 124, 10712–10729, https://doi.org/10.1029/2019JD031243. 499 Dubache, G., B. A. Ogwang, V. Ongoma, and A. R. Md. Towfigul Islam, 2019: The effect of 500 Indian Ocean on Ethiopian seasonal rainfall. Meteorology and Atmospheric Physics, 131, 501 1753–1761, https://doi.org/10.1007/s00703-019-00667-8. 502 Endris, H. S., C. Lennard, B. Hewitson, A. Dosio, G. Nikulin, and G. A. Artan, 2019: Future 503 changes in rainfall associated with ENSO, IOD and changes in the mean state over Eastern 504 Africa. Climate Dynamics, 52 2029–2053, https://doi.org/10.1007/s00382-018-4239-7. 505 Farrow, A., D. Musoni, S. Cook, and R. Buruchara, 2011: Assessing the risk of root rots in 506 common beans in East Africa using simulated, estimated and observed daily rainfall data. 507 Experimental Agriculture, 47, 357–373, https://doi.org/10.1017/S0014479710000980. 508 Funk, C., and Coauthors, 2015: The climate hazards infrared precipitation with stations—a new 509 environmental record for monitoring extremes. Scientific Data, 2, 510 https://doi.org/10.1038/sdata.2015.66. 511 Gleixner, S., N. Keenlyside, E. Viste, and D. Korecha, 2017: The El Niño effect on Ethiopian 512 summer rainfall. Climate Dynamics, 49, 1865–1883, https://doi.org/10.1007/s00382-016-513 3421-z.

- Hartter, J., M. D. Stampone, S. J. Ryan, K. Kirner, C. A. Chapman, and A. Goldman, 2012:
- Patterns and perceptions of climate change in a biodiversity conservation hotspot. *PLoS*
- 516 *ONE*, 7, e32408, https://doi.org/10.1371/journal.pone.0032408.
- Hastenrath, S., and D. Polzin, 2004: Dynamics of the surface wind field over the equatorial
- Indian Ocean. Quarterly Journal of the Royal Meteorological Society, 130, 503–517,
- 519 <a href="https://doi.org/10.1256/qj.03.79">https://doi.org/10.1256/qj.03.79</a>.
- Herrmann, S. M., and K. I. Mohr, 2011: A continental-scale classification of rainfall seasonality
- regimes in Africa based on gridded precipitation and land surface temperature products.
- *Journal of Applied Meteorology and Climatology*, **50**, 2504–2513,
- 523 <u>https://doi.org/10.1175/JAMC-D-11-024.1</u>.
- Hoell, A., and C. Funk, 2013: The ENSO-related West Pacific sea surface temperature gradient.
- *Journal of Climate*, **26**, 9545–9562, <a href="https://doi.org/10.1175/JCLI-D-12-00344.1">https://doi.org/10.1175/JCLI-D-12-00344.1</a>.
- Hua, W., L. Zhou, H. Chen, S. E. Nicholson, A. Raghavendra, and Y. Jiang, 2016: Possible
- 527 causes of the Central Equatorial African long-term drought. *Environmental Research Letters*,
- 528 **11**, 124002, https://doi.org/10.1088/1748-9326/11/12/124002.
- King, J. A., R. Washington, and S. Engelstaedter, 2020: Representation of the Indian Ocean
- Walker circulation in climate models and links to Kenyan rainfall. *International Journal of*
- *Climatology*, <a href="https://doi.org/10.1002/joc.6714">https://doi.org/10.1002/joc.6714</a>.
- Lau K-M, and S. Yang, 2015: Walker circulation. Encyclopedia of Atmospheric Sciences, G.R.
- North, J. Pyle, and F. Zhang, Eds, Elsevier, 177–181.
- Levin, N. E., E. J. Zipser, and T. E. Cerling, 2009: Isotopic composition of waters from Ethiopia
- and Kenya: Insights into moisture sources for eastern Africa. *Journal of Geophysical*
- 536 Research, 114, https://doi.org/10.1029/2009JD012166.

- 537 Liebmann, B., I. Bladé, G. N. Kiladis, L. M. V. Carvalho, G. B. Senay, D. Allured, S. Leroux,
- and C. Funk, 2012: Seasonality of African Precipitation from 1996 to 2009. Journal of
- 539 *Climate*, **25**, 4304–4322, <a href="https://doi.org/10.1175/JCLI-D-11-00157.1">https://doi.org/10.1175/JCLI-D-11-00157.1</a>.
- 540 —, and Coauthors, 2014: Understanding recent eastern Horn of Africa rainfall variability and
- 541 change. *Journal of Climate*, **27**, 8630–8645, <a href="https://doi.org/10.1175/JCLI-D-13-00714.1">https://doi.org/10.1175/JCLI-D-13-00714.1</a>.
- Lyon, B., 2014: Seasonal drought in the Greater Horn of Africa and its recent increase during the
- March–May long rains. Journal of Climate, 27, 7953–7975, https://doi.org/10.1175/JCLI-D-
- 544 13-00459.1.
- MacLeod, D., R. Graham, C. O'Reilly, G. Otieno, and M. Todd, 2021: Causal pathways linking
- different flavours of ENSO with the Greater Horn of Africa short rains. *Atmospheric Science*
- 547 *Letters*, **22**, e1015, <a href="https://doi.org/10.1002/asl.1015">https://doi.org/10.1002/asl.1015</a>.
- Maidment, R. I., and Coauthors, 2017: A new, long-term daily satellite-based rainfall dataset for
- operational monitoring in Africa. *Scientific Data*, 4, <a href="https://doi.org/10.1038/sdata.2017.63">https://doi.org/10.1038/sdata.2017.63</a>.
- Marshall, J., A. Donohoe, D. Ferreira, and D. McGee, 2014: The ocean's role in setting the mean
- position of the Inter-Tropical Convergence Zone. Climate Dynamics, 42, 1967–1979,
- 552 https://doi.org/10.1007/s00382-013-1767-z.
- Mélice, J.-L., and J. Servain, 2003: The tropical Atlantic meridional SST gradient index and its
- relationships with the SOI, NAO and Southern Ocean. *Climate Dynamics* 20, 447–464,
- 555 <u>https://doi.org/10.1007/s00382-002-0289-x.</u>
- Monaghan, A. J., K. MacMillan, S. M. Moore, P. S. Mead, M. H. Hayden, and R. J. Eisen, 2012:
- A regional climatography of West Nile, Uganda, to support human plague modeling. *Journal*
- of Applied Meteorology and Climatology, **51**, 1201–1221, https://doi.org/10.1175/JAMC-D-
- 559 11-0195.1.

560 Mutai, C. C., and M. N. Ward, 2000: East African rainfall and the tropical circulation/convection 561 on intraseasonal to interannual timescales. *Journal of Climate*, 13, 3915–3939, 562 https://doi.org/10.1175/1520-0442(2000)013<3915:EARATT>2.0.CO;2. 563 Ngecu, W. M., and E. M. Mathu, 1999: The El-Nino-triggered landslides and their 564 socioeconomic impact on Kenya. Environmental Geology, 38, 277–284, https://doi.org/10.1007/s002540050425. 565 566 Nicholson, S. E., 2014: A detailed look at the recent drought situation in the Greater Horn of 567 Africa. Journal of Arid Environments, 103, 71–79, 568 https://doi.org/10.1016/j.jaridenv.2013.12.003. 569 – 2015: Long-term variability of the East African 'short rains' and its links to large-scale 570 factors. International Journal of Climatology, 35, 3979–3990, 571 https://doi.org/10.1002/joc.4259. 572 — 2017: Climate and climatic variability of rainfall over eastern Africa. *Reviews of* 573 Geophysics, 55, 590–635, https://doi.org/10.1002/2016RG000544. 574 —— 2018: The ITCZ and the seasonal cycle over equatorial Africa. *Bulletin of the American* Meteorological Society, 99, 337–348, https://doi.org/10.1175/BAMS-D-16-0287.1. 575 576 Nicholson, S., 2000: The nature of rainfall variability over Africa on time scales of decades to 577 millenia. Global and Planetary Change, 26, 137–158, https://doi.org/10.1016/S0921-578 8181(00)00040-0. 579 —, and J. Kim, 1997: The relationship of the El Niño–Southern Oscillation to African rainfall. International Journal of Climatology, 17, 117–135, https://doi.org/10.1002/(SICI)1097-580 581 0088(199702)17:2<117::AID-JOC84>3.0.CO;2-O.

582 —, and A. K. Dezfuli, 2013: The relationship of rainfall variability in western equatorial 583 Africa to the tropical oceans and atmospheric circulation. Part I: The boreal spring. Journal 584 of Climate, 26, 45–65, https://doi.org/10.1175/JCLI-D-11-00653.1. 585 Okonya, J. S., K. Syndikus, and J. Kroschel, 2013: Farmers' perception of and coping strategies 586 to climate change: evidence from six agro-ecological zones of Uganda. Journal of 587 Agricultural Science, 5, 252–263, https://doi.org/10.5539/jas.v5n8p252. 588 Omondi, P., L. A. Ogallo, R. Anyah, J. M. Muthama, and J. Ininda, 2013: Linkages between 589 global sea surface temperatures and decadal rainfall variability over Eastern Africa region. 590 International Journal of Climatology, 33, 2082–2104, https://doi.org/10.1002/joc.3578. 591 Osbahr, H., P. Dorward, R. Stern, and S. Cooper, 2011: Supporting agricultural innovation in 592 Uganda to respond to climate risk: linking climate change and variability with farmer 593 perceptions. Experimental Agriculture, 47, 293–316, 594 https://doi.org/10.1017/S0014479710000785. 595 Reynolds, R. W., N. A. Rayner, T. M. Smith, D. C. Stokes, and W. Wang, 2002: An improved in 596 situ and satellite SST analysis for climate. *Journal of Climate*, 15, 1609–1625, 597 https://doi.org/10.1175/1520-0442(2002)015<1609:AIISAS>2.0.CO;2. 598 Roncoli, C., K. Ingram, and P. Kirshen, 2002: Reading the rains: local knowledge and rainfall 599 forecasting in Burkina Faso. Society & Natural Resources, 15, 409-427, 600 https://doi.org/10.1080/08941920252866774. 601 Roncoli, C., B. S. Orlove, M. R. Kabugo, and M. M. Waiswa, 2011: Cultural styles of 602 participation in farmers' discussions of seasonal climate forecasts in Uganda. Agriculture and 603 Human Values, 28, 123–138, https://doi.org/10.1007/s10460-010-9257-y.

604 Saji, N. H., B. N. Goswami, P. N. Vinayachandran, and T. Yamagata, 1999: A dipole mode in 605 the tropical Indian Ocean. *Nature*, **401**, 360–363, https://doi.org/10.1038/43854. 606 Salerno, J., J. E. Diem, B. L. Konecky, and J. Hartter, 2019: Recent intensification of the 607 seasonal rainfall cycle in equatorial Africa revealed by farmer perceptions, satellite-based 608 estimates, and ground-based station measurements. Climatic Change, 153, 123–139, 609 https://doi.org/10.1007/s10584-019-02370-4. 610 Schott, F. A., S.-P. Xie, and J. P. McCreary, 2009: Indian Ocean circulation and climate 611 variability. Reviews of Geophysics, 47, https://doi.org/10.1029/2007RG000245. 612 Schreck, C. J., and F. H. M. Semazzi, 2004: Variability of the recent climate of eastern Africa. 613 International Journal of Climatology, 24, 681–701, https://doi.org/10.1002/joc.1019. 614 Segele, Z. T., P. J. Lamb, and L. M. Leslie, 2009: Seasonal-to-interannual variability of 615 Ethiopia/Horn of Africa monsoon. Part I: Associations of wavelet-filtered large-scale 616 atmospheric circulation and global sea surface temperature. Journal of Climate, 22, 3396-617 3421, https://doi.org/10.1175/2008JCLI2859.1. 618 Ssempiira, J., J. Kissa, B. Nambuusi, E. Mukooyo, J. Opigo, F. Makumbi, S. Kasasa, and P. Vounatsou, 2018: Interactions between climatic changes and intervention effects on malaria 619 620 spatio-temporal dynamics in Uganda. Parasite Epidemiology and Control, 3, e00070, 621 https://doi.org/10.1016/j.parepi.2018.e00070. 622 Todd, M. C., and R. Washington, 2004: Climate variability in central equatorial Africa: 623 Influence from the Atlantic sector. Geophysical Research Letters, 31, 624 https://doi.org/10.1029/2004GL020975. 625 UNMA, 2021. Seasonal Forecasts. Accessed 19 March 2021. https://www.unma.go.ug/seasonal-

626

forecasts/

627 Vellinga, M., and S. F. Milton, 2018: Drivers of interannual variability of the East African "Long 628 Rains." Quarterly Journal of the Royal Meteorological Society, 144, 861–876, 629 https://doi.org/10.1002/qj.3263. 630 Webster, P.J., 2004. The elementary Hadley circulation. The Hadley Circulation: Present, Past 631 and Future, H.F. Diaz and R.S. Bradley, Eds, Springer, 9-60. 632 Wenhaji Ndomeni, C., E. Cattani, A. Merino, and V. Levizzani, 2018: An observational study of 633 the variability of East African rainfall with respect to sea surface temperature and soil 634 moisture. Ouarterly Journal of the Royal Meteorological Society, 144, 384–404, 635 https://doi.org/10.1002/qj.3255. 636 Wilkie, D., G. Morelli, F. Rotberg, and E. Shaw, 1999: Wetter isn't better: Global warming and 637 food security in the Congo Basin. Global Environmental Change, 9, 323–328, 638 https://doi.org/10.1016/S0959-3780(99)00021-7. 639 Zougmoré, R. B., S. T. Partey, M. Ouédraogo, E. Torquebiau, and B. M. Campbell, 2018: Facing 640 climate variability in sub-Saharan Africa: analysis of climate-smart agriculture opportunities 641 to manage climate-related risks. Cahiers Agricultures, 27, 34001, 642 https://doi.org/10.1051/cagri/2018019.

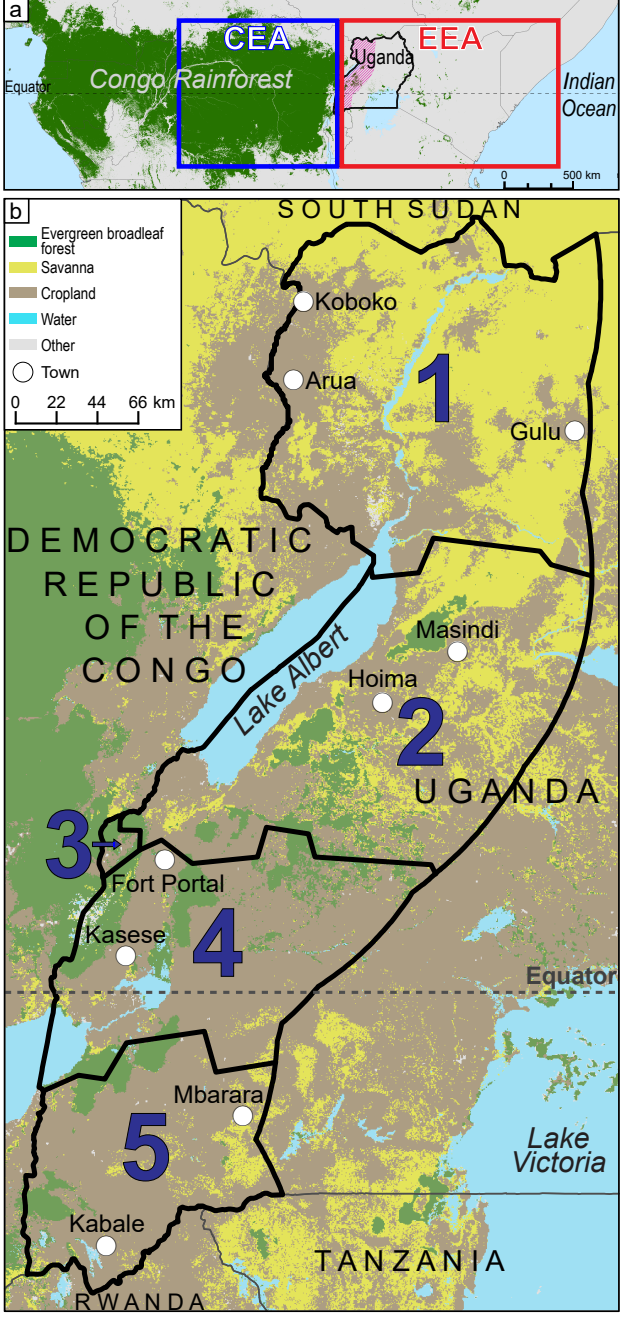


FIG. 1. (a) Location of the western Uganda study area, a zone within 160-km of the Congo Basin (Diem et al. 2019a), with respect to the Congo rainforest, central equatorial Africa (CEA), and eastern equatorial Africa (EEA). (b) The five rainfall regions, major towns, and the dominant land-cover types in western Uganda. Land-cover information is derived from the MODIS land-cover type product (MCD12Q1).

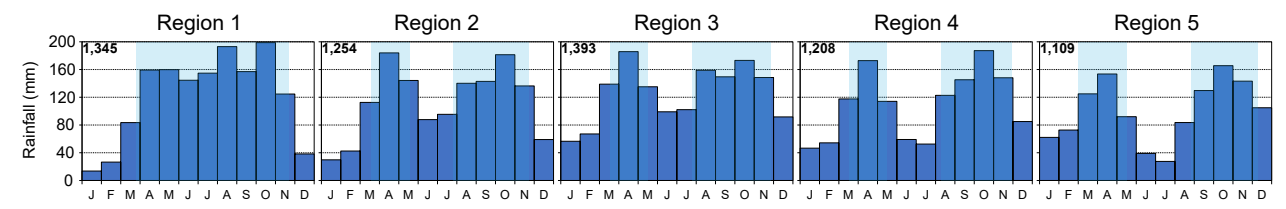


FIG. 2. Mean monthly rainfall totals over 1983-2019 for the five rainfall regions. Annual rainfall totals (in mm) are shown in the upper-left corner of each panel. Approximate rainy-season periods are shown with blue shading. The mean of CHIRPS and TAMSAT data were used to estimate rainfall totals (see Section 3 for a description of the satellite-based rainfall data). Rainy-season information is based on information in Figure 2 in Diem et al. (2019b).

FIG. 3. Locations of the 10 regions from which tropical SST indices are calculated. Western Uganda is highlighted in color. In addition to the Niño indices in the central and eastern equatorial Pacific Ocean are the following: the North Atlantic Tropical (NAT) index, the South Atlantic Tropical (SAT) index, the Western Tropical Indian Ocean (WTIO) index, the Southeastern Tropical Indian Ocean (SETIO) index, and the Western Pacific (WP) index. The indices are described in Section 3.

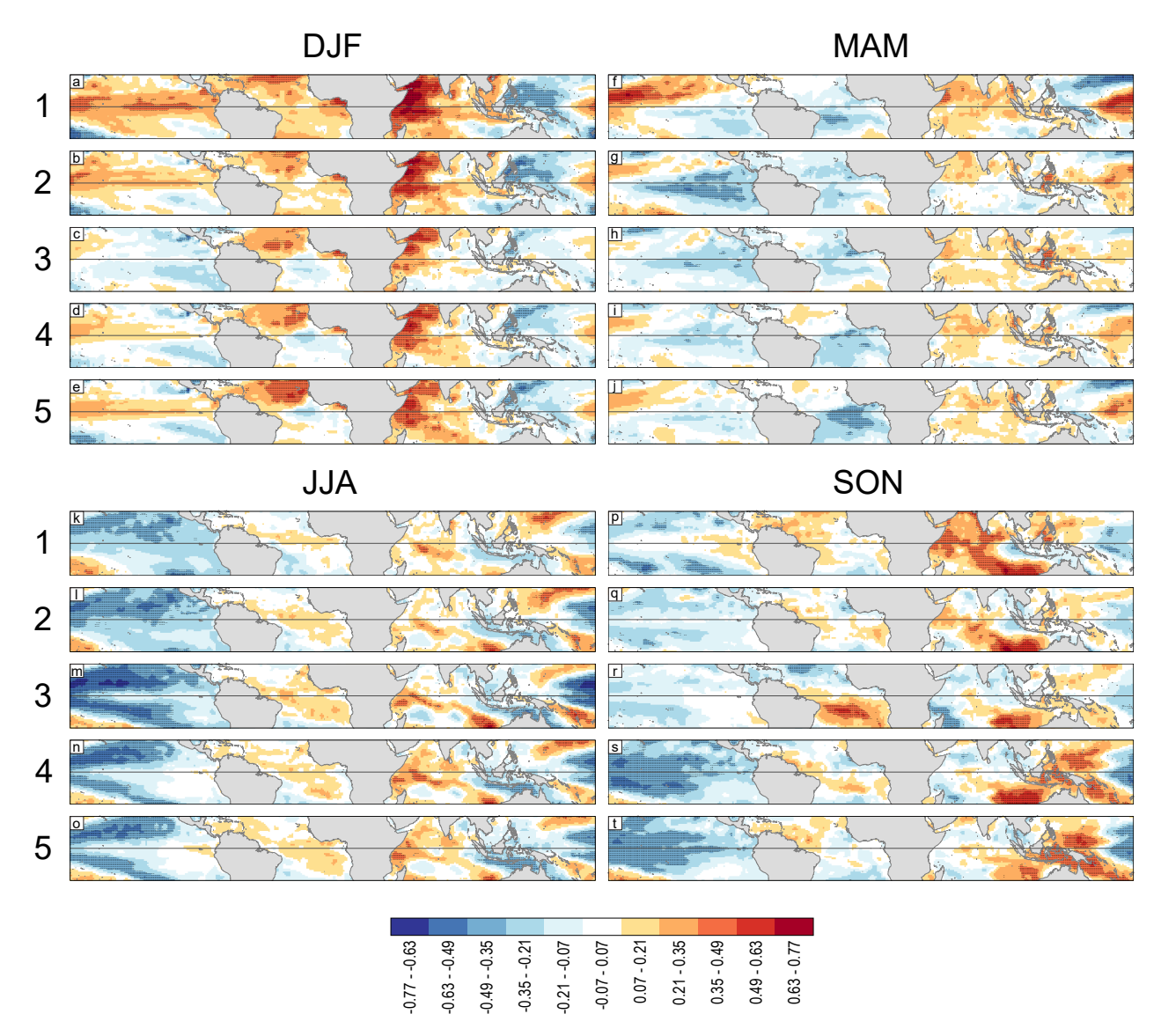


FIG. 4. Sea-surface temperature (SST) correlations for the five rainfall regions of western Uganda for (a-e) December-February (DJF), (f-j) March-May (MAM), (k-o) June-August (JJA), and (p-t) September-November (SON). Stippling indicates significant ( $\alpha$  = 0.05; two-tailed) correlations between rainfall and SSTs.

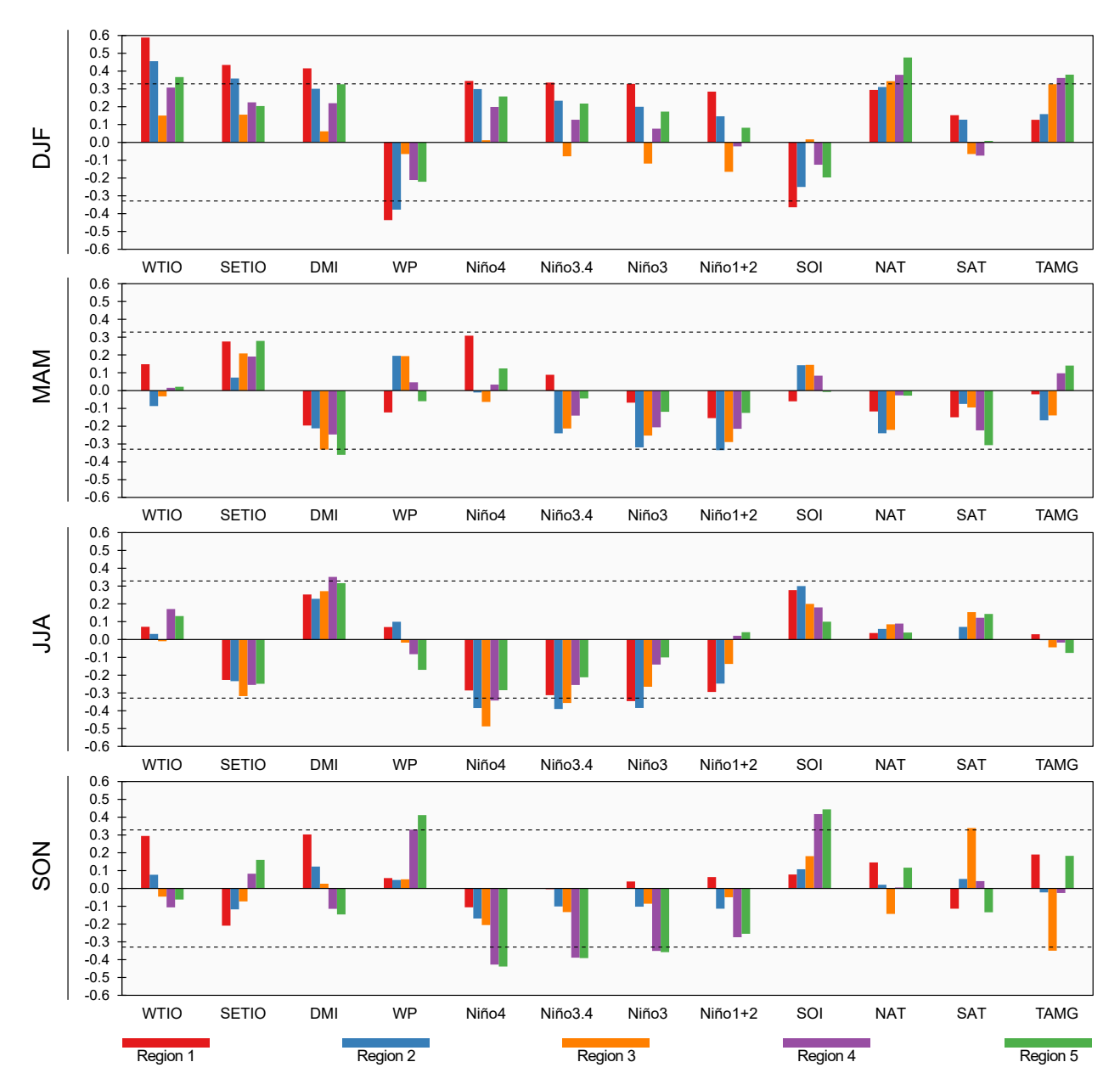


FIG. 5. Correlations between regional rainfall and the 12 indices for the four climatological seasons. Bars extending beyond the dashed lines indicate significant ( $\alpha$ = 0.05; one-tailed) correlations. The indices are described in Section 3.

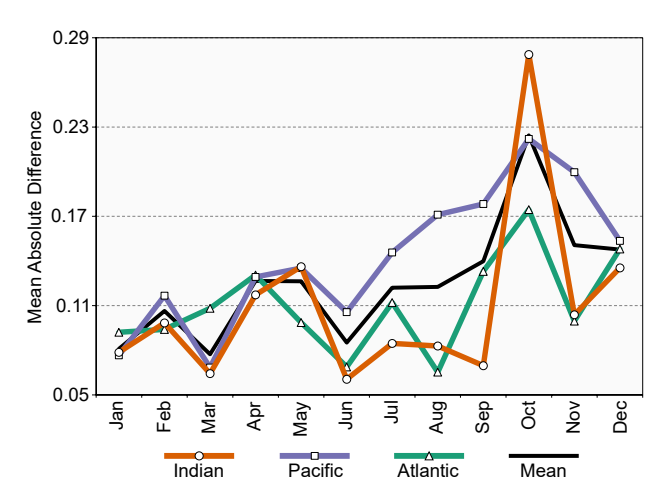


FIG. 6. Intra-annual variations in mean absolute differences in SST correlations among the five rainfall regions. The values for each ocean basin are the mean of the absolute differences in correlation coefficients for each index for each pair of rainfall regions.

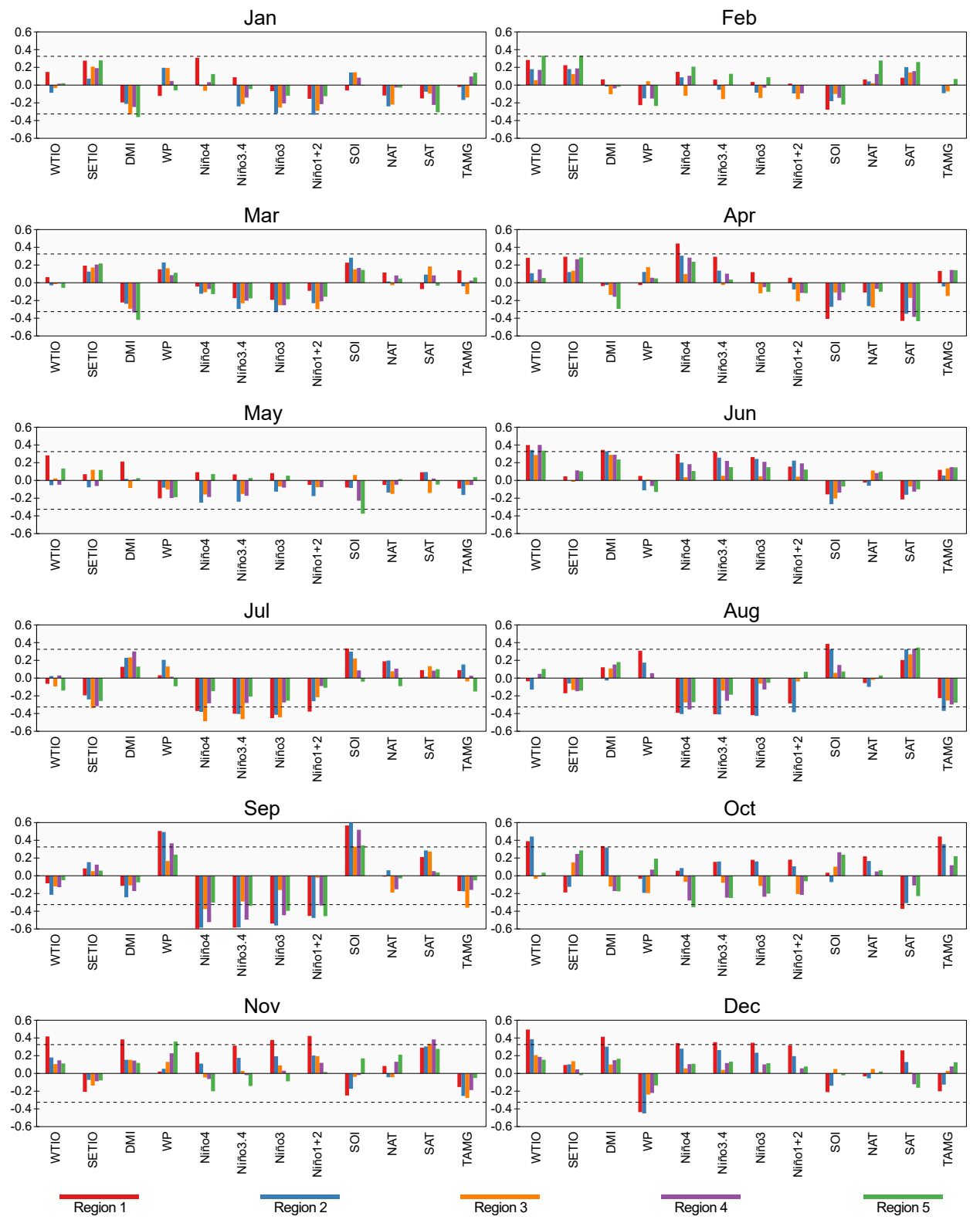


FIG. 7. Correlations between regional rainfall and the 12 indices for each month. Bars extending beyond the dashed lines indicate significant ( $\alpha$ = 0.05; two-tailed) correlations. The indices are described in Section 3.

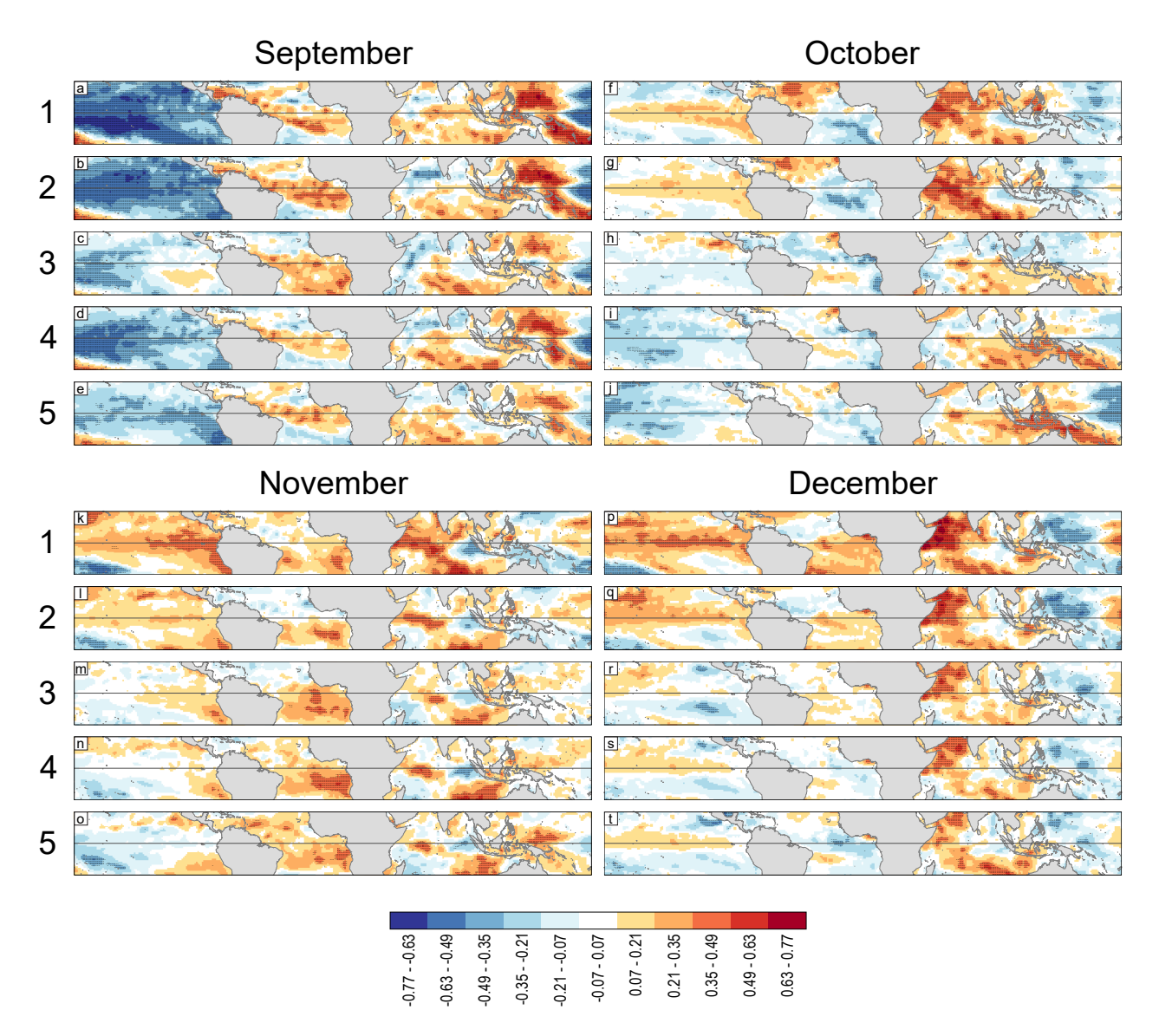


FIG. 8. Sea-surface temperature (SST) correlations for the five rainfall regions of western Uganda for (a-e) September, (f-j) October, (k-o) November, and (p-t) December. Stippling indicates significant ( $\alpha = 0.05$ ; two-tailed) correlations between rainfall and SSTs.